MOLECULAR AND CELLULAR BIOLOGY, Dec. 2005, p. 10492–10506 Vol. 25, No. 23
0270-7306/05/$08.00+0 doi:10.1128/MCB.25.23.10492–10506.2005

Werner Protein Protects Nonproliferating Cells from Oxidative DNA Damage†

Anna M. Szekely,[1,2] Franziska Bleichert,[1] Astrid Nümann,[1]‡ Stephen Van Komen,[1] Elisabeth Manasanch,[1]¶ Abdelhakim Ben Nasr,[1]§ Allon Canaan,[1] and Sherman M. Weissman[1]*

Department of Genetics[1] and Department of Neurology,[2] Yale University School of Medicine, New Haven, Connecticut 06510

Received 1 December 2004/Returned for modification 10 January 2005/Accepted 31 August 2005

Werner syndrome, caused by mutations of the *WRN* gene, mimics many changes of normal aging. Although roles for WRN protein in DNA replication, recombination, and telomere maintenance have been suggested, the pathology of rapidly dividing cells is not a feature of Werner syndrome. To identify cellular events that are specifically vulnerable to WRN deficiency, we used RNA interference (RNAi) to knockdown WRN or BLM (the RecQ helicase mutated in Bloom syndrome) expression in primary human fibroblasts. Withdrawal of WRN or BLM produced accelerated cellular senescence phenotype and DNA damage response in normal fibroblasts, as evidenced by induction of γH2AX and 53BP1 nuclear foci. After WRN depletion, the induction of these foci was seen most prominently in nondividing cells. Growth in physiological (3%) oxygen or in the presence of an antioxidant prevented the development of the DNA damage foci in WRN-depleted cells, whereas acute oxidative stress led to inefficient repair of the lesions. Furthermore, WRN RNAi-induced DNA damage was suppressed by overexpression of the telomere-binding protein TRF2. These conditions, however, did not prevent the DNA damage response in BLM-ablated cells, suggesting a distinct role for WRN in DNA homeostasis in vivo. Thus, manifestations of Werner syndrome may reflect an impaired ability of slowly dividing cells to limit oxidative DNA damage.

Among the simple Mendelian disorders of humans, Werner syndrome most closely resembles an acceleration of normal aging (20, 32). Although the distribution of lesions is somewhat atypical for normal aging, Werner patients show osteoporosis, atherosclerosis, thinning of skin, graying of hair, cataracts and diabetes (33). Peripheral insulin resistance appears to precede the diabetes, as it does in maturity onset type II diabetes in the general population. Werner syndrome has attracted the interest of a number of investigators because of the hope that understanding its pathogenesis could shed light on the molecular weak links in normal aging.

The gene mutated in Werner syndrome encodes the WRN protein, a 3′-5′ DNA helicase of the RecQ family that also exhibits exonuclease activity (for a review, see references 25, 35, and 37). WRN has been suggested to function in DNA replication and repair. The helicase is capable of unwinding various DNA structures such as D-loops and G-quartets, and various structures potentially associated with progressing replication forks, as well as promoting migration of Holliday junctions such as might be formed as intermediates in DNA recombination. WRN can directly interact with a variety of proteins involved in these processes, including the major DNA polymerase, polymerase delta; polymerase beta, a DNA polymerase used in base excision repair; the Ku complex; the FEN1 nuclease that removes single-stranded branch structures in DNA; and the p53 DNA checkpoint gene. Previous studies reported slow progression of S phase in cells from Werner patients and proposed that fewer origins of replication are used and/or that the replication fork progresses more slowly or asymmetrically than in normal cells, suggesting that the disorder somehow affects DNA replication (42). Selective sensitivity of Werner cells to 4-nitroquinoline was reported some time ago, and more recent studies have extended the range of sensitivity to include topoisomerase inhibitors such as camptothecin, as well as some DNA cross-linking reagents (for a review, see reference 25). Also, a series of genetic and molecular studies have been interpreted to suggest that there are abnormalities in DNA recombination in Werner cells. WRN has been suggested to play a role in suppressing excessive recombination by removing or reversing recombinational intermediates. WRN interacts with the Ku protein that functions in nonhomologous DNA end joining and with Nbs1 that is a part of the Mre11 complex functioning in homologous recombination. The abnormalities produced by lack of WRN or of the yeast homolog Sgs1 may be alleviated by interfering with the function of Rad51, the homolog of *Escherichia coli* RecA, a central player in homologous recombination (for a review, see reference 35). Consistent with this, cells

* Corresponding author. Mailing address: Department of Genetics, Yale University School of Medicine, TAC Bldg., Rm. S319, 300 Cedar St., New Haven, CT 06510. Phone: (203) 737-2282. Fax: (203) 737-2286. E-mail: sherman.weissman@yale.edu.

† Supplemental material for this article may be found at http://mcb.asm.org/.

‡ Present address: Institut für Neuropathologie, Charité-Humboldt Universität, Campus Virchow-Klinikum, Augustenburger Platz 1, D-13353 Berlin, Germany.

¶ Present address: University of Barcelona, Tapineria 10, 2, 08002 Barcelona, Spain.

§ Present address: Department of Immunology and Microbiology, University of Texas Medical Branch, 301 University Blvd., Galveston, TX 77555.

from Werner patients show a variegated pattern of chromosomal rearrangements (23, 47).

The Werner protein is also implicated in telomere maintenance. Transfection of constructs expressing telomerase can immortalize and partly correct the 4-nitroquinoline sensitivity of Werner cells (26, 60). The telomere-binding protein TRF2 binds to WRN and stimulates WRN activity in vitro (39). Interestingly, mice lacking a functional WRN gene are relatively normal, but very recent reports show that significant portions of the Werner syndrome can be reproduced experimentally when, in WRN knockout mice, the telomeres are shortened as a consequence of inactivation of telomerase (8, 31).

Mutations in the related RecQ helicase BLM protein produces Bloom syndrome, a disorder that shares relatively limited features with Werner syndrome (19). The helicase activities of WRN and BLM proteins overlap considerably in substrate specificity, as does the set of proteins each helicase interacts with in vivo or in vitro, and WRN and BLM proteins can directly associate with one another (56). Mutations in another RecQ helicase, RecQL4, produces disorders with phenotypes that are also quite distinct from Werner syndrome (30, 50).

The cell biologic bases for the difference in phenotypes of these disorders and for the overlap between effects of WRN loss and normal aging are unknown. Also, a primary role for WRN in DNA replication and recombination would not explain the observed pattern of abnormalities in Werner patients. For example, it is not clear how the peripheral insulin resistance relates to DNA replication, and abnormalities in some of the most rapidly dividing cell types such as hematopoietic cells and the gastrointestinal mucosa are not prominent parts of the Werner syndrome. In addition, most of the studies of the cellular effects of deprivation of WRN have been based either on cells that might have undergone adaptation or selection for viability in vitro or in cells from individuals in whom in vivo adaptations might have occurred.

There are a number of DNA helicases encoded in the genome and several potentially complementary ways to avoid or repair DNA damage. It is at least possible that the normal role for WRN protein might be different or more significant than is suggested from studies of cells derived from an organism with germ line mutation thus adapted to grow in the absence of WRN. To understand the relationship between the molecular abnormality in cells lacking WRN and the consequent specific organismal phenotype, it would be useful to identify cellular events that are vulnerable to WRN deficiency but not to BLM deficiency. We have used RNA interference (RNAi) (18) to knock down endogenous WRN and BLM in various cell types without subsequent selection for propagating cells. The consequences of WRN depletion are more dramatic than the defects in cells derived from Werner patients, suggesting that the latter cells have undergone a functional compensation for WRN deficiency. We show here that in primary human fibroblasts withdrawal of WRN leads to accelerated development of a cellular phenotype that is consistent with checkpoint activation such as occurs in replicative senescence. Acute loss of WRN leads to DNA damage in normal fibroblasts, as evidenced by development of an established DNA damage response, the accumulation of γH2AX and 53BP1 nuclear foci (22, 34). Nondividing WRN-depleted cells are particularly prone to accumulate DNA damage, in contrast to the effects of BLM depletion. We also show that physiological (3%) oxygen level, addition of an antioxidant to the culture, or overexpression of the telomere-associated protein TRF2 prevented the occurrence of acute WRN-loss induced DNA damage foci in asynchronous cells, as well as in cells arrested in the G_1 phase of the cell cycle. These effects are different from those seen in BLM-depleted cells. We suggest that defects in DNA repair of specific lesions produced by oxidative damage in slowly dividing or nondividing cells account for those aspects of the Werner syndrome that mimic normal aging.

MATERIALS AND METHODS

Cell lines, culture conditions, and cell cycle synchronization. Primary WI-38 and IMR-90 fibroblasts (obtained from the American Type Culture Collection and the Coriell Institute for Medical Research) were grown in standard tissue culture conditions at ambient oxygen levels unless indicated otherwise and maintained in Dulbecco modified Eagle medium (DMEM) supplemented with 15% fetal bovine serum (FBS), 2 mM glutamine, and 0.1 mM nonessential amino acids. The experiments were performed at population doublings (PDL) 24 to 27 unless indicated otherwise. Early-passage WI-38 and IMR90 cells were at PDL 12, with late passages at PDL 42 to 46. The simian virus 40 (SV40) transformed WI-38 cells (Coriell) were cultured by using DMEM–10% FBS. Controlled low-oxygen conditions were established by using a continuous flow (1 liter/min) of a humidified mixture of 3% O_2, 92% N_2, and 5% CO_2 gas (premixed and certified by Airgas Northeast) to a fully sealed metal chamber maintained at 37°C (41). The cells were maintained in this environment throughout and removed only briefly (<5 min) from this chamber for the necessary medium change or treatment. Quiescent (G_0) populations of WI-38 cells were obtained by culturing the cells in DMEM containing 0.5% FBS for 72 h before harvesting. To arrest the cells at G_1, after the small interfering RNA (siRNA) transfection the cells were maintained in DMEM containing 0.5% FBS for 72 h and then incubated for 24 h using DMEM–20% FBS in the absence or presence of 20 μM R-roscovitine (Calbiochem). To arrest the cells at confluence, the initial plating and transfections were performed at high density (~80% confluence), and the cell density was subsequently monitored. The general upstream caspase inhibitor Z-VAD-FMK was obtained from Trevigen. To induce acute oxidative stress, primary WI-38 cells were cultured under 3% oxygen. At 96 h after siRNA introduction the cells were treated with various doses H_2O_2 in a serum free-medium for 45 min. For time course experiments, the medium was changed after the treatment to DMEM containing 10% FBS, and the cells were allowed to recover at 3% O_2 for various amounts of time. In experiments to reduce chronic oxidative injury, the cells were subcultured at ambient oxygen in the presence of 100 μM *N-t*-butyl hydroxylamine (NtBHA; Aldrich) (1) for 2 weeks before siRNA transfection experiments began.

siRNA preparation, RNAi-resistant plasmid generation, and transfections. To design target specific siRNA duplexes, we selected sequences of the type AA (N_{19}) UU from the open reading frame of the targeted mRNAs, followed by an extensive BLAST search against the human genome sequence to maximally increase the likelihood that only one gene is targeted. The 21-nucleotide (nt) RNAs were either chemically synthesized (Keck Facility, Yale University) and then deprotected, desalted, and annealed or were purchased from Dharmacon (Lafayette, CO), as was the nonspecific scrambled (SCR) control duplex. After testing of several siRNA constructs for their knockdown efficiency, in the experiments presented here we used duplexes targeting the following sequences: for human Werner syndrome mRNA (NM_000533), 5′-AACTGTATCTTCGGG CACCAA-3′; for the human Bloom syndrome mRNA (NM_00057) (BLM), 5′-AACGAACTGCTTCAGCAGCGG-3′; and for a scrambled siRNA, 5′-GCG CGCTTTGTAGGATTCGdTdT-3′. Exponentially growing primary fibroblasts (~30% confluence) were siRNA transfected with Oligofectamine (Invitrogen), while in experiments requiring transfection at high-density (~80% confluence), Metafectene (Biontix) was used, both according to the manufacturer's instructions. The transfection efficiency and time course were evaluated by fluorescence and phase-contrast microscopy using fluorescein isothiocyanate (FITC)- and Cy3-tagged WRN and and FITC-tagged GL3 siRNAs. Site-directed mutagenesis of the full-length WRN and BLM cDNAs were performed by the QuickChange II XL system (Stratagene). The primer sequences were selected against the siRNA targeted regions of the respective genes by changing critical nucleotides that are essential for RNAi-mediated degradation of mRNAs (18) but without altering protein coding properties of the encoded mRNA. The region described above targeted by WRN siRNA was changed to AAC**G**GTATCT**AGC**GG

CACCAA (mutagenized nucleotides are in boldface); the targeted BLM region was changed to AACGA**GCTCTTG**CAGCAGCGG. Forward and reverse primers for the RNAi-resistant WRN cDNA, both containing the desired mutations, were 5′-CTGCCTAGTTCGAAAACGGTATCTAGCGGCACCAAAGAGCATTG-3′ and 5′-CAATGCTCTTTGGTGCCGCTAGATACCGTTTTCGAACTAGGCAG-3′, respectively. For the BLM RNAi-resistant cDNAs, the forward and reverse primers were 5′-GGATTGTGGGAACGAGCTCTTGCAGCAGCGGAACATAAGAAGG-3′ and 5′-CCTTCTTATGTTCCGCTGCTGCAAGAGCTCGTTCCCACAATCC-3′, respectively. After primer extension with Pfu Ultra DNA polymerase (Stratagene), the plasmids were digested with DpnI endonuclease to select for mutation-containing plasmids. The recovered mutated full-length WRN and BLM cDNAs, originally cloned into pcDNA3.1/Hygro bearing a C terminus TAP tag and pEGFP-C terminus tag vectors, respectively, were isolated, and the mutations were confirmed by sequencing. The full-length TRF2 and DN-TRF2 (pADhTRF2-myc 3′ and pADmychTRF2DN) were kindly provided by Titia de Lange. When sequential transfection of plasmids and siRNAs were performed, at 16 to 24 h after splitting the cells were transfected with the various full-length cDNAs, followed by an additional 16 h of culture and transfection of siRNAs with Metafectene (Biontix), for both steps according to the manufacturer's instructions. The experimental schedules are presented separately.

RNA isolation and real-time RT-PCR. Total RNA was isolated by the RNeasy protocol (QIAGEN). First-strand cDNA was prepared from 500 ng of total RNA with gene specific primers and *C. thermophilus* polymerase for reverse transcription (RT; Roche) in a final reaction volume of 10 μl. Dilutions of the respective cDNAs synthesized from total RNA of untreated WI-38 cells were used to establish external standard curves. Real-time PCR amplifications were performed with gene-specific primer sets in an iCycler apparatus (Bio-Rad). Quantification of a given mRNA, expressed as relative mRNA level compared to the transfection reagent (mock control), was calculated after normalization to GAPDH (glyceraldehyde-3-phosphate dehydrogenase) mRNA expression by using both the standard curve and the $\Delta\Delta C_T$ formula. Individual values were derived from triplicate measurements, and at least three independent biological experiments were performed. The specificity of the PCR amplification was verified by melting-curve analysis of the final products and by agarose-gel electrophoresis.

Cell cycle analysis and apoptosis assays. Cell-cycle progression was analyzed by propidium iodide staining and FACScan analysis (Becton Dickinson). Cell viability, apoptosis, and necrosis of WI-38 cells were evaluated 4 or 5 days after the respective siRNA transfections by double staining for Alexa 488-conjugated annexin V and propidium iodide, followed by fluorescence-activated cell sorting (FACS) analysis, all according to the manufacturer's recommendations (Molecular Probes).

SA-β-Gal assay. The cells were plated in 24-well plates and fixed with 3% formaldehyde. Senescence-associated β-galactosidase (SA-β-Gal) was assayed at pH 6.0 as described previously (15). The images of three randomly selected fields per each well were analyzed either with a Nikon Eclipse TS100 inverted microscope by using bright-field and phase-contrast microscopy or, for cells cultured on glass coverslips, a Nikon Eclipse 800 fluorescence microscope with bright-field illumination for evaluation for galactosidase activity and visualization of DNA by DAPI (4′,6′-diamidino-2-phenylindole) counterstaining using fluorescence microscopy. At least 300 cells for each condition were analyzed, and the data were obtained from a minimum of five independent biological experiments.

Immunoblotting. Whole-cell lysates were prepared by using either Laemmli sample buffer (ca. 10^4 cells/μl) or radioimmunoprecipitation assay buffer, fractionated on sodium dodecyl sulfate-polyacrylamide gel electrophoresis, transferred onto polyvinylidene difluoride or Nitrocellulose membranes, and probed. Blocking and incubation with primary antibodies were performed in 5% milk–0.1% Tween 20 in phosphate-buffered saline (PBS). The antibodies used were rabbit anti-WRN polyclonal antibody (pAb) and anti-BLM pAb (Novus); anti-p16 and anti-pRB monoclonal antibodies (MAbs; BD Biosciences); anti-Phospho-Rb (Se780) pAb and anti-Phospho-p53 (Se20 pAb and Se15 MAb)(Cell Signaling); anti-p53 MAb (DO-1; Oncogene Research); anti-p21 MAb, anti-TRF2 pAb, and antivimentin MAb (Santa Cruz); and anti-γ-tubulin (Sigma). After incubations with horseradish peroxidase-linked secondary antibodies (Amersham), all blots were developed by using chemiluminescence detection (Pierce ECL). Quantification of the data was performed by using densitometric analysis of the autoradiographs (Quantity One software; Bio-Rad). The expression of WRN and BLM proteins were normalized relative to the expression of the structural proteins vimentin or γ-tubulin that served as loading controls.

Immunofluorescence analysis. Cells were cultured directly on glass coverslips, fixed with either 4% formaldehyde or 3% paraformaldehyde for 10 min in PBS, and permeabilized by 0.1% Triton X-100 for 15 min at room temperature or 0.2% Triton X-100 for 20 min on ice for detection of BLM and γH2AX or 53BP1, respectively. Coverslips were blocked either by 1% bovine serum albumin–0.1% Triton X-100 or 0.2% cold water fish gelatin–0.5% bovine serum albumin. The conditions of subsequent primary antibody incubation for BLM, γH2AX, and 53BP1 staining were described previously (7, 48, 53). The phosphohistone H3 (Ser10) immunostaining was performed according to the manufacturer's recommendations. Primary antibodies were as follows: anti-BLM pAb (Novus and Abcam), γH2AX MAb (Upstate Biotechnology), and phosphohistone H3 (Se10; Cell Signaling). 53BP1 MAb was kindly provided by Thanos Halazonetis. Alexa-488 and Alexa-594 anti-rabbit and Alexa-488 anti-mouse secondary antibodies were from Molecular Probes. Images of control and experimental cells were acquired with identical exposure conditions and analyzed by using a Nikon Eclipse E800 fluorescence microscope using Compix software. Quantification of nuclear foci was determined from a minimum of 250 cells for each experimental point and in at least three independent biological experiments. Cells were scored as "focus positive" if more than 6 foci (with an average size of 1 μm) per nucleus were present for γH2AX and more than 10 foci for 53BP1, respectively, with minimum ×40 magnification used. The percentage of focus-positive cells in the cell population is presented for experiments characterizing the effect of knockdowns in various conditions. However, to compare various approaches (i.e., siRNA transfection by Oligofectamine versus double transfection of siRNA and cDNAs using another reagent and temporal sequence, for instance), the results are normalized and expressed as fold changes in the fraction of focus-positive cells. The normalization was performed comparing the percent of focus-positive cells of the condition (i.e., various siRNA transfections) to the percentage of focus-positive cells in the presence of the respective transfection reagent (Oligofectamine or Metafectene) alone, serving as baseline for the given experimental set up. For pairwise comparisons Student *t* test was used for statistical analysis.

RESULTS

Acute loss of RecQ helicases WRN and BLM leads to accelerated senescence in primary human fibroblasts. To investigate the effects of acute depletion of WRN or the related RecQ helicase BLM in human cells, we used RNAi (18) to target the relevant genes in human fibroblasts. Using fluorescein dye-tagged 21-bp double-stranded siRNAs we confirmed that the transfection efficiency depended on time and dose with an average of 70% at 50 nM siRNA concentrations. The siRNA persisted for at least 5 days in either primary WI-38 fibroblasts or its SV40 transformed line (data not shown). We identified siRNA constructs that significantly reduced WRN or BLM mRNA and protein expression and that lack significant homology with the other human RecQ helicases and to other expressed genes (Fig. 1). The rate of decline of WRN protein level is a function of the protein stability and in this setting it took 3 to 4 days for extensive reduction of the levels of WRN protein (Fig. 1A). The overall depletion of at least 70% with a minimum of 70% transfection efficiency suggests that the depletion ranged from complete depletion in 70% of the cells to 70% depletion in 100% of the cells. Quantitative, real-time RT-PCR measurements showed that WRN mRNA expression displayed an average reduction of ca. 70% as early as 2 days after siRNA transfection (Fig. 1D, left panel). Importantly, targeting of these related RecQ helicases was specific, since the mRNA level of the homologous BLM gene was unaffected by WRN siRNA (Fig. 1D, left panel). siRNA-mediated targeting of BLM led to a significant decrease of BLM protein expression by 4 days posttransfection (Fig. 1B) and of the characteristic pattern of nucleoplasmic BLM immunoreactivity (36) in primary fibroblasts (Fig. 1C). BLM siRNA decreased BLM, but not WRN mRNA expression (Fig. 1D, right panel). These data indicate that RNAi oc-

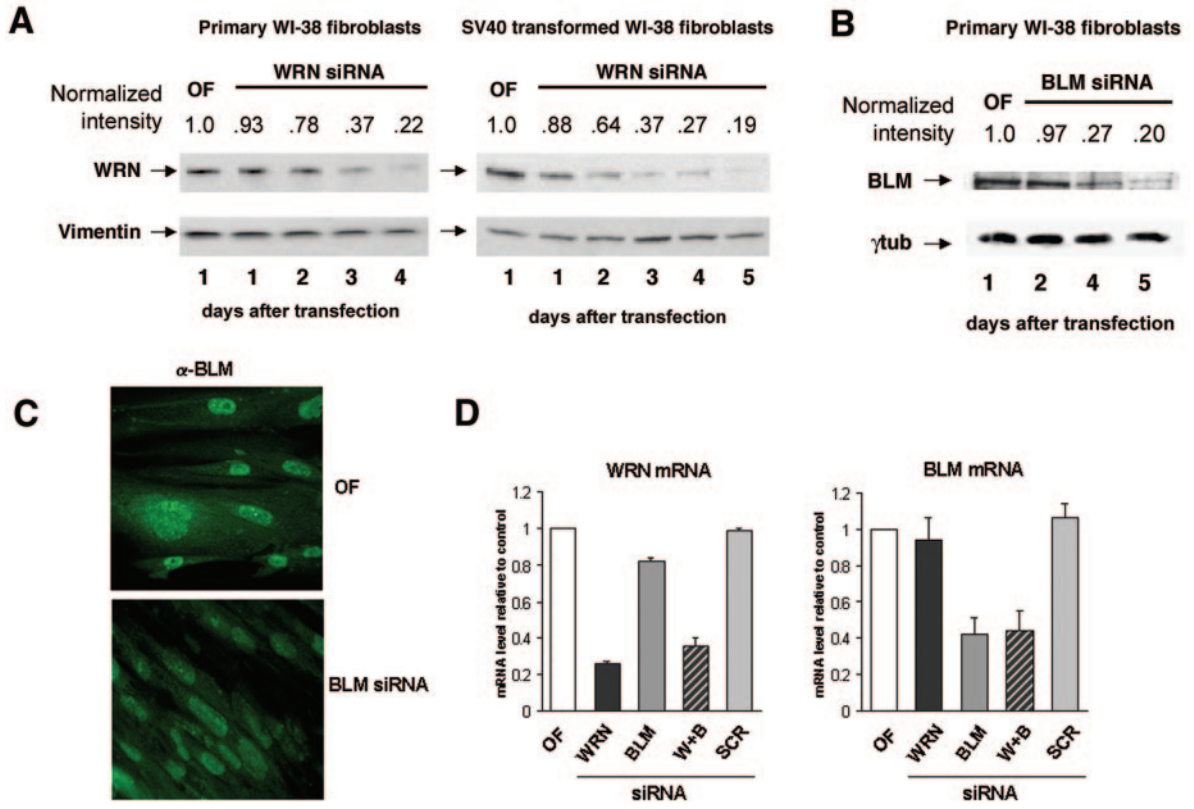

FIG. 1. Acute knockdown of WRN and BLM expression by RNA interference in primary human fibroblasts. (A) Immunoblot analysis showing the specific decrease of WRN protein in primary (PDL 25) and SV40-transformed WI-38 fibroblasts. The cells were transfected with a synthetic siRNA duplex targeting WRN (for details, see Materials and Methods) and whole-cell extracts were generated at the indicated time points. The expression of vimentin remained stable throughout the time course and was used for a loading control for the Western blot. Quantification of immunoblots is shown. Signal intensities for WRN and for the vimentin bands were divided by intensities of their respective mock-transfected (Oligofectamine) controls, and the calculated normalized intensities for WRN expression are indicated. OF, Oligofectamine mock transfection. (B) Time-dependent decline of BLM protein expression after siRNA transfection targeting *BLM* in primary WI-38 fibroblasts (PDL 26). γ-Tubulin was used as a loading control. Quantification of the immunoblot was performed as described above. (C) Immunofluorescence microscopy shows decreased BLM expression evidenced by the decreased diffuse nucleoplasmic stain and loss of disperse punctate nuclear foci in WI-38 primary fibroblasts 4 days after transfection with siRNA targeting *BLM* anti-BLM pAb (green). (D) Specificity of siRNAs repressing WRN and BLM mRNA expression. Quantitative real-time RT-PCR was performed 2 days after various siRNA transfections, as indicated. SCR represents scrambled siRNA control. A total of 500 ng of total RNA was used for the RT and gene-specific primers encompassing the regions targeted by the respective siRNAs for PCR amplification. GAPDH mRNA expression remained stable throughout the experimental schedule and was used as reference control. The histograms represent the fold changes normalized to GAPDH and mock transfection (OF). The results are from three independent experiments done in triplicates; error bars show the standard error of mean (SEM).

curred with high efficiency and specificity in primary untransformed fibroblasts.

Primary fibroblasts from Werner patients have a reduced life span in vitro before entering replicative senescence (46). We found that upon withdrawal of WRN, the morphology of untransformed primary fibroblasts changed progressively within 5 days posttransfection. The cells became enlarged, flattened and developed the SA-β-Gal activity (15) with a concomitant moderate decline of cumulative cell number (Fig. 2A and B). The senescent fraction showed an additional increase of 8 to 10% from day 5 to day 7 after WRN siRNA transfection (data not shown). The growth characteristics and morphology of cells were unaltered by a scrambled siRNA construct that does not target human genes. Only a fraction of primary fibroblasts showed SA-β-Gal staining, perhaps a limitation in the detection method or a reflection of heterogeneity in the cellular response. These effects were dose dependent (significant effects required 5 to 10 nM siRNA), were seen following simultaneous knockdown of *WRN* and *BLM* genes, and were observed in two different primary fibroblast lines (WI-38 and IMR90), as well as in early-passage (PDL 12) or late-passage (PDL 45) cells, arguing against cell line specificity or dependence on a distinct presenescent stage (data not shown). RNAi directed against BLM resulted in a similar or somewhat greater reduction in cell number and appearance of SA-β-Gal activity, albeit with less evident flattening morphology of the cells (Fig. 2A and B). The corresponding siRNA transfections in SV40-transformed fibroblasts produced growth arrest without evidence of senescent morphology or the induction of SA-β-Gal activity seen with the untransformed cells (data not shown).

Untransformed fibroblasts responded to acute knockdown of WRN with a minimal elevation of the levels of p21, the downstream p53 target, and the p16 cell-cycle inhibitors within

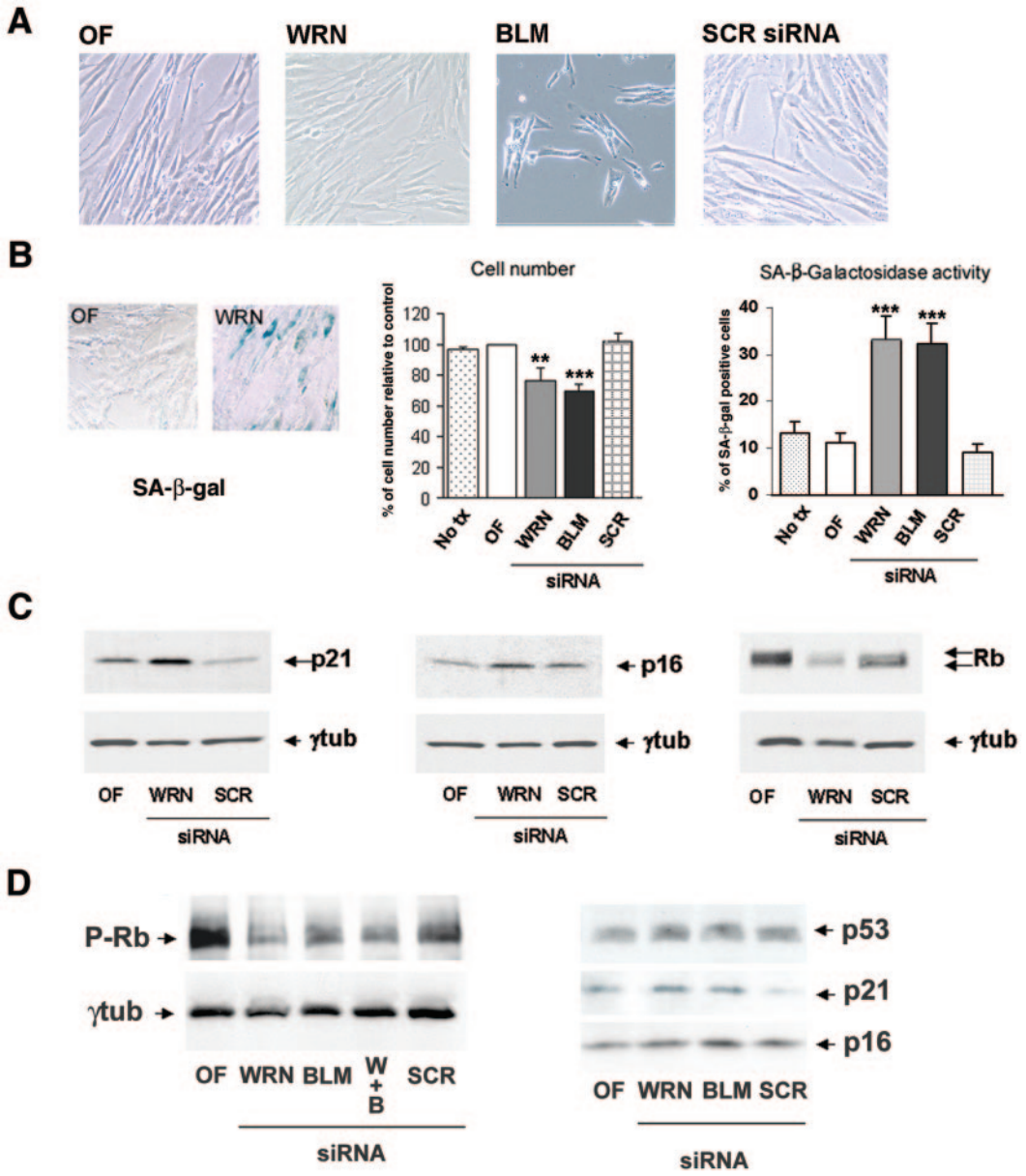

FIG. 2. Senescence response in primary fibroblasts after siRNA-mediated depletion of WRN and BLM. (A) Morphological changes induced by RNAi in primary fibroblasts. WI-38 cells (at PDL 24) were transfected with various siRNAs as indicated and were photographed under phase contrast microscopy 4 days later. Magnification, ×40. (B) RNAi targeting of WRN and BLM induces SA-β-Gal activity (SA-β-gal). Representative photographs of WI-38 cells stained for SA-β-Gal 4 days after mock (Oligofectamine [OF]) and WRN siRNA transfection are shown. The lower panel shows the quantitation of cell number and proportion of SA-β-Gal-positive cells 4 days after transfection with various siRNAs, as indicated. Experiments were performed at PDL 24 to 26. Histograms indicate the cell count in percentage normalized to cells treated with the transfection reagent only (left panel) and the percentage of SA-β-Gal positive cells (right panel). On average more than 300 cells were analyzed per datum point per experiment and data derived from at least five independent biological experiments. Error bars representing the SEM are shown. Statistical analysis using Student *t* test was performed. Statistically significant differences compared to respective OF controls are indicated: **, $P < 0.01$; ***, $P < 0.001$. (C and D) Effect of WRN (C) and BLM (D) depletion on the p53 and pRb pathways. Immunoblot analyses were performed with total cell lysates prepared 5 days after siRNA transfections. The concentration of the siRNAs was 50 nM; when WRN was combined with BLM knockdown, a 25 nM concentration of each siRNA was used. The hyperphosphorylated form of pRb protein is indicated as a doublet using an anti-Rb antibody (Rb) that recognizes both the modified and the unmodified protein. Phospho-specific Rb antibody (P-Rb) was used to directly analyze the phosphorylated fraction of Rb. γ-Tubulin served as loading control.

the time frame of 5 days (Fig. 2C and D, right panel). However, an almost complete disappearance of retinoblastoma (Rb) phosphorylation and, to a lesser degree, the dephosphorylated Rb protein was evident (Fig. 2C and D, left panel). We found essentially no change in p53 protein levels after WRN knockdown, although there was a 2.5-fold increase in p53 mRNA level by microarray analysis (Fig. 2D, right panel, and unpublished data). Furthermore, when total cellular lysates were

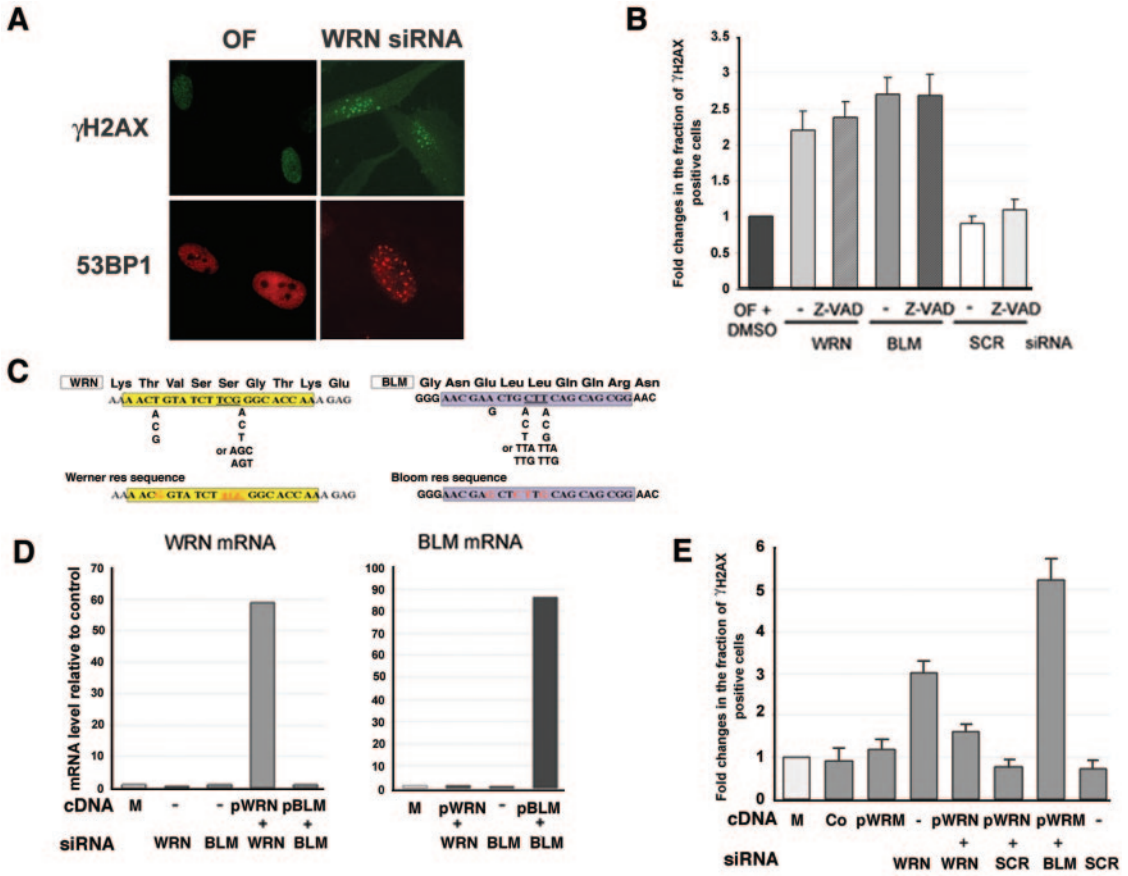

FIG. 3. Accumulation of the DNA damage foci γH2AX and 53BP1 by acute withdrawal of WRN and BLM in WI-38 primary fibroblasts. (A) Primary WI-38 cells (PDL 26) at ~30% confluence were transfected with the various siRNAs and cultured in the presence of 10% serum. At 4 days posttransfection, immunofluorescence analysis for γH2AX and 53BP1 foci was performed. The figure shows representative patterns of γH2AX and 53BP1 foci formation after WRN RNAi using anti-γH2AX and 53BP1 mouse MAbs (green and red, respectively). OF, Oligofectamine. (B) γH2AX foci accumulation by acute WRN and BLM depletion in the presence of the general caspase inhibitor Z-VAD-FMK. The cells were grown in the presence of 20 μM Z-VAD-FMK from the time of siRNA transfection as described in Fig. 2. Histograms indicate the percentage of cells with γH2AX foci in primary, asynchronous WI-38 cells after various siRNA transfections, as indicated. On average, more than 250 intact nuclei were screened per individual condition, and the data represent the means and SEMs of triplicate samples. (C) Generation of RNAi-resistant full-length WRN and BLM cDNAs by site-directed mutagenesis. The targeted sequences highlighted and the mutagenized nucleotides are indicated in boldface. (D) Specificity of the WRN and BLM RNAi-resistant full-length cDNA constructs. Real time RT-PCR was performed after sequential transfections. After 16 to 24 h of cell splitting, the cells were transfected with the various cDNAs, followed by siRNA transfection within 16 h, as indicated. Total RNA was isolated after 36 h of the siRNA transfections. (E) Complementation of the WRN siRNA-induced DNA damage response by RNAi-resistant full-length WRN gene. Sequential transfections were performed as described above. The cells were fixed 4 days after siRNA transfections, as indicated. The percentage of γH2AX-positive cells expressed as the fold changes compared to the value of the control cells treated the transfection reagent, Metafectene (M), alone. Error bars represent the SEMs of three experiments. Co-V, control expression plasmid; pWRN, RNAi-resistant full-length WRN cDNA; SCR, scrambled siRNA control.

tested by using commercial phospho-specific p53 antibodies against Se15 or Se20, we were not able to detect phosphorylation of p53 at 4 and 5 days after introduction of WRN siRNA (data not shown). Acutely BLM-depleted cells also showed marked dephosphorylation of Rb protein and marginal changes in p21 and p16 expression within 5 days (Fig. 2D).

The significant hypophosphorylation of Rb was accompanied by decreased proliferation of the WRN-deficient cells, as evidenced by an average 40% reduction of bromodeoxyuridine incorporation (data not shown) and a similar decrease in S-phase cells with an increased proportion of G_0-G_1 cells by FACS analysis (see Fig. S1A in the supplemental material). Furthermore, using an antibody that specifically recognizes the phophorylated form of histone H3, present exclusively in mitosis, the mitotic indices of the WRN and BLM depleted cells were significantly decreased (see Fig. S1B in the supplemental material).

Several measures indicated that decreases in cell number were not due in major part to the induction of apoptosis. The proportion of the WRN-RNAi-treated cells with apoptotic/necrotic features, as assessed by morphological criteria of nuclear blebbing or fragmentation after DAP1 stain and <2N DNA content by FACS analysis, was not significantly different from the mock-transfected or nonspecific siRNA-transfected controls groups (data not shown). Furthermore, the general upstream caspase inhibitor Z-VAD-FMK did not alter the changes in cell number seen after WRN or BLM RNAi (see Fig. S2A in the supplemental material). In addition, cells were

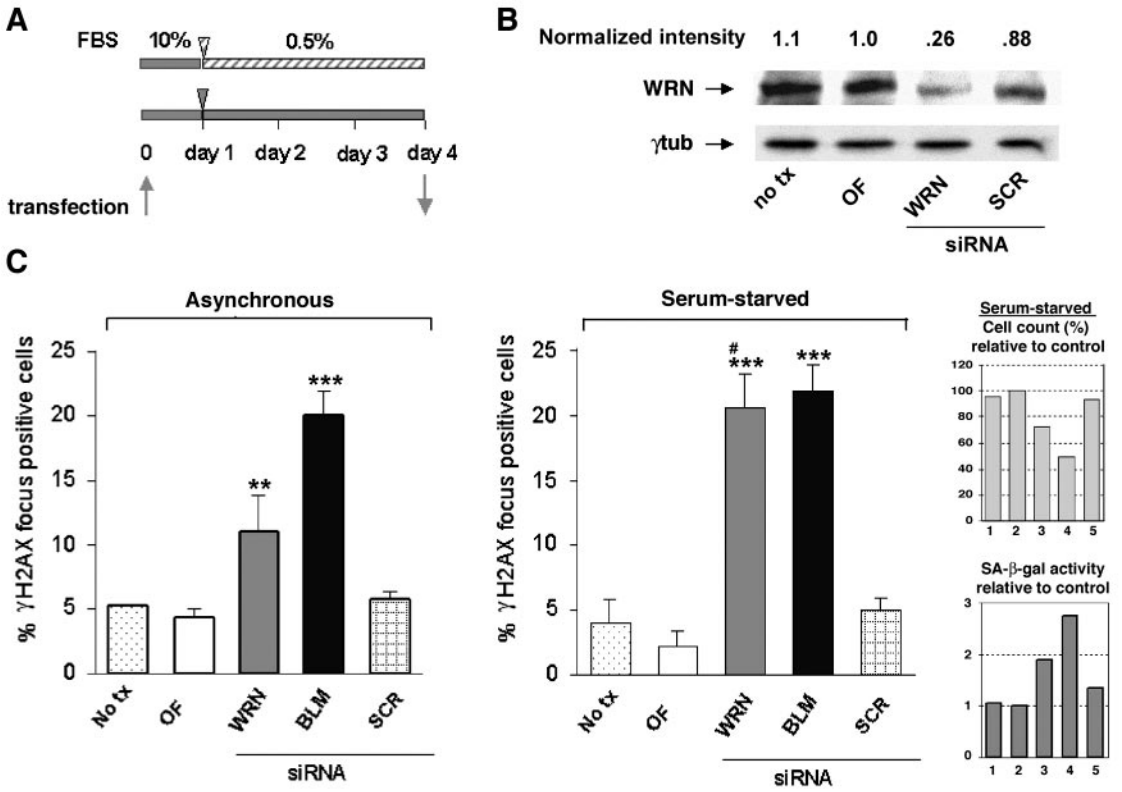

FIG. 4. Preferential accumulation of DNA damage foci by acute withdrawal of WRN in serum-synchronized cells. (A) Primary WI-38 cells (PDL 26) at ~30% confluence were transfected with the various siRNAs and either cultured in the presence of 10% serum (asynchronous) or synchronized with 0.5% serum for 72 h to put the cell into the G_0 state, as shown by the experimental time line. (B) Quantitative immunoblot analysis (as described in the legend to Fig. 1) shows the extent of WRN depletion at day 4 posttransfection in serum-starved WI-38 cells. The concentration of the various siRNAs was 50 nM. (C) Quantitation of γH2AX foci. Histograms indicate the percentage of cells with foci (for criteria, see Materials and Methods) in primary asynchronous (left panel) or serum synchronized (right panel) WI-38 cells 4 days after various siRNA transfections. On average, more than 250 intact nuclei were screened per individual condition, and the data were derived from at least four independent biological experiments. Error bars represent the SEM. **, level of significance with a P value of <0.05; ***, level of significance with a P value of <0.005 (compared to the respective OF control was made by using Student t test). The "#" symbol indicates a statistically significant difference ($P < 0.05$) in γH2AX foci formation between serum-synchronized and asynchronous WRN depleted cells. The inset shows the cell number and SA-β-Gal expression in serum-synchronized cells after RNAi; the average of two independent experiments is shown. Columns: 1, no treatment; 2, OF, 3, WRN siRNA; 4, BLM siRNA; 5, SCR siRNA. OF, Oligofectamine.

stained and analyzed by FACS for annexin as a surface marker for apoptotic cells and propidium iodide for necrosis. There was only a minor increase in the apoptotic fraction and negligible changes in the number of necrotic cells after transfection with either WRN or BLM siRNAs compared to cells treated with a scrambled siRNA or Oligofectamine alone (see Fig. S2B in the supplemental material).

Together, these results suggest that acute depletion of WRN or BLM under standard culture conditions largely inhibited cell growth, produced evidence of cellular senescence, and resulted in checkpoint activation, even in early-passage primary fibroblasts. Moreover, the phenotypic consequences of acute WRN depletion appeared more dramatic than those seen in cells derived from Werner patients.

Acute knockdown of WRN, but not BLM, results in augmented DNA damage in nonreplicating primary cells. The in vitro studies of enzymatic activities of WRN and BLM protein and their in vitro and in vivo protein associations all implicate these proteins in DNA transactions such as those involved in DNA replication and recombinational repair (25). We considered it likely that the cellular senescence seen in WRN-depleted cells was due to defects in DNA transactions leading to accumulation of DNA damage. As a surrogate marker for DNA damage, we examined the formation of nuclear foci containing phosphorylated H2AX (γH2AX) and the p53 binding protein 1 (53BP1). It is well established that in response to DNA double-stranded breaks (DSBs) H2AX is rapidly phosphorylated by upstream kinases in the chromatin microenvironment flanking the site of DNA damage, facilitating the focal assembly of checkpoint and DNA repair factors in many somatic cells, including human diploid fibroblasts (7, 43, 44). In asynchronous cells, immunofluorescence studies revealed a significant increase in the percentage of cells showing γH2AX foci after WRN RNAi and an even more extensive formation of foci in acutely BLM-depleted cells (Fig. 3A and Fig. 4C, left panel). Time course analysis revealed that the peak level of γH2AX focus formation was seen at 4 days in both WRN and BLM knockdown cells (see Fig. S3 in the supplemental material).

53BP1 is a BRCT motif-containing protein that responds

rapidly to different types of DNA damage. It is a key transducer of the DNA damage checkpoint signaling and, together with the other damage sensor protein γH2AX, has been shown to accumulate at sites of DNA breaks (48, 59). After RNAi-mediated WRN knockdown, 53BP1-containing foci accumulated in the nuclei of primary fibroblasts, similarly to the induction of γH2AX foci (Fig. 3A). To address whether γH2AX foci might also mark sites of DNA DSBs as a sequel to apoptosis, the cells were maintained from the time of the siRNA transfection in a medium containing a general upstream caspase inhibitor peptide Z-VAD-FMK. The WRN and BLM RNAi-induced DNA damage response, monitored by γH2AX focus formation, was identical in the absence or presence of Z-VAD-FMK (Fig. 3B). Annexin staining of cells also showed that there was only a small increase in the fraction of apoptotic cells after RNAi, and this increase did not correlate with the increase in H2AX foci (see Fig. S2B in the supplemental material). These findings suggest that phosphorylation of H2AX reflects DNA lesions that are generated primarily by the functional absence of WRN and BLM in DNA transactions. In addition, cDNA profiling revealed that at least 20 genes, whose products are intimately involved in repairing various DNA lesions, had significantly elevated mRNA levels in primary fibroblasts following WRN RNAi (A. M. Szekely et al., unpublished results).

To further substantiate the specificity of our approach, we performed complementation experiments using the RNAi-mediated DNA damage response as a biological readout. We modified critical nucleotides of the siRNA-targeted regions of full-length WRN and BLM cDNAs by mutagenesis to create RNAi-resistant genes, without altering their protein coding properties (Fig. 3C). Transfection of these modified full-length cDNAs elicited a significant, specific increase of their respective mRNA levels in the presence of the targeting siRNAs, and an increase in the level of the specific protein (Fig. 3D and data not shown). Overexpression of WRN and BLM in normal fibroblasts did not alter cellular growth properties or result in toxicity (data not shown). Importantly, overexpression of the RNAi-resistant full-length WRN led to a nearly complete rescue of the WRN but not accumulation of BLM siRNA-induced γH2AX foci (Fig. 3E), thus confirming the specificity of the siRNA-mediated endogenous gene silencing.

Since WRN has been suggested to be involved in processes related to DNA replication, we studied the effects of cell cycle synchronization by serum starvation on WRN or BLM-depleted cells (Fig. 4A). The extent of siRNA-mediated WRN depletion using this synchronization approach was comparable to that seen in asynchronous cells (Fig. 4B and Fig. 1A). Quantitative analyses revealed that the fraction of γH2AX foci-positive cells was significantly increased in cells grown in 0.5% serum after WRN RNAi compared to the asynchronously grown WRN-deficient cells (Fig. 4C). This augmented induction was also evident when the cells were plated in low-serum medium before siRNA transfection (data not shown), suggesting that γH2AX focus formation is not restricted to cells that have divided after being depleted of WRN. On the other hand, serum starvation did not change the extent of γH2AX foci development in cells with reduced BLM levels (Fig. 4C). The senescence response in serum-synchronized WRN and BLM knockdown cells was also evident (Fig. 4C, inset).

To further investigate the effect of cell cycle progression on the development of DNA damage foci, we used roscovitine, a well-studied inhibitor of cyclin-dependent kinases, to produce G_1 arrest (49). After siRNA transfection, the cells were synchronized with 0.5% serum for 3 days and then treated with roscovitine for 24 h in the presence of 20% serum-containing medium (Fig. 5A). FACS analysis of DNA content of the cells confirmed that this treatment significantly decreased the number of S-phase cells in control and WRN- or BLM-depleted cells (see Fig. S4A in the supplemental material). Quantitative immunoblotting confirmed that the extent of WRN depletion in the roscovitine-synchronized cells is similar to that of seen in asynchronous cells (Fig. 5B). Similar to previous studies (17), we found that the endogenous level of BLM protein is poorly expressed in arrested cells (data not shown). Real-time RT-PCR verified a 56% decrease of BLM mRNA expression at day 5 posttransfection in the roscovitine-synchronized cells. After roscovitine synchronization, primary fibroblasts with WRN withdrawal displayed a further increase of γH2AX foci formation in comparison to asynchronous populations. In contrast, after roscovitine synchronization there was a decline in the fraction of focus-positive cells subsequent to BLM RNAi (Fig. 5C). Roscovitine treatment itself did not block either the development of foci or the appearance of features of senescence after RNAi (Fig. 5C, inset), even though the roscovitine-sensitive kinase CDK5 contributes to cellular senescence in a human osteosarcoma cell line (61). Furthermore, a third method of replication arrest was achieved by confluence (Fig. 5D). Confluent cells showed a very similar profile of DNA damage foci accumulation to that seen with roscovitine arrest. The cell cycle distributions were comparable using these various synchronization approaches. Furthermore, apoptosis/necrosis analysis by annexin and propidium iodide staining of G_0-G_1 arrested cells by serum starvation, roscovitine synchronization, and confluence showed only a minor increase in the apoptotic fraction compared to the low (on average 2 to 3%) baseline of the control siRNA-transfected cells (see Fig. S4A and B in the supplemental material).

Taken together, the results show that acute loss of endogenous WRN and BLM leads to rapid development of DNA damage in primary cells. The disappearance of phosphorylated H2AX foci after DNA damage is normally rather rapid, occurring with a half-life of few hours (43). Therefore, progression through S phase is not required for γH2AX foci formation. Our data indicate that acute WRN depletion results in DNA damage that accumulates particularly in nonreplicating primary fibroblasts, most likely due to continuing DNA damage. The divergent responses after acute WRN and BLM loss show that G_1 synchronization dissociates the functions of WRN and BLM helicases.

Physiological (3%) oxygen level prevents the development of DNA damage response induced by acute WRN loss. Oxidative damage, including double-stranded DNA lesions and telomeric damage, has been proposed to play a causative role in organismal aging (3, 28, 40). Standard cell culture systems include more than six times the physiological cellular oxygen tension (149 mm Hg/ambient 20% O_2 versus 23 mm Hg/3% O_2); hence, DNA damage is thought to be induced chronically by reactive oxygen species (28). This could result directly in DSBs or create lesions that are converted to DSB after DNA

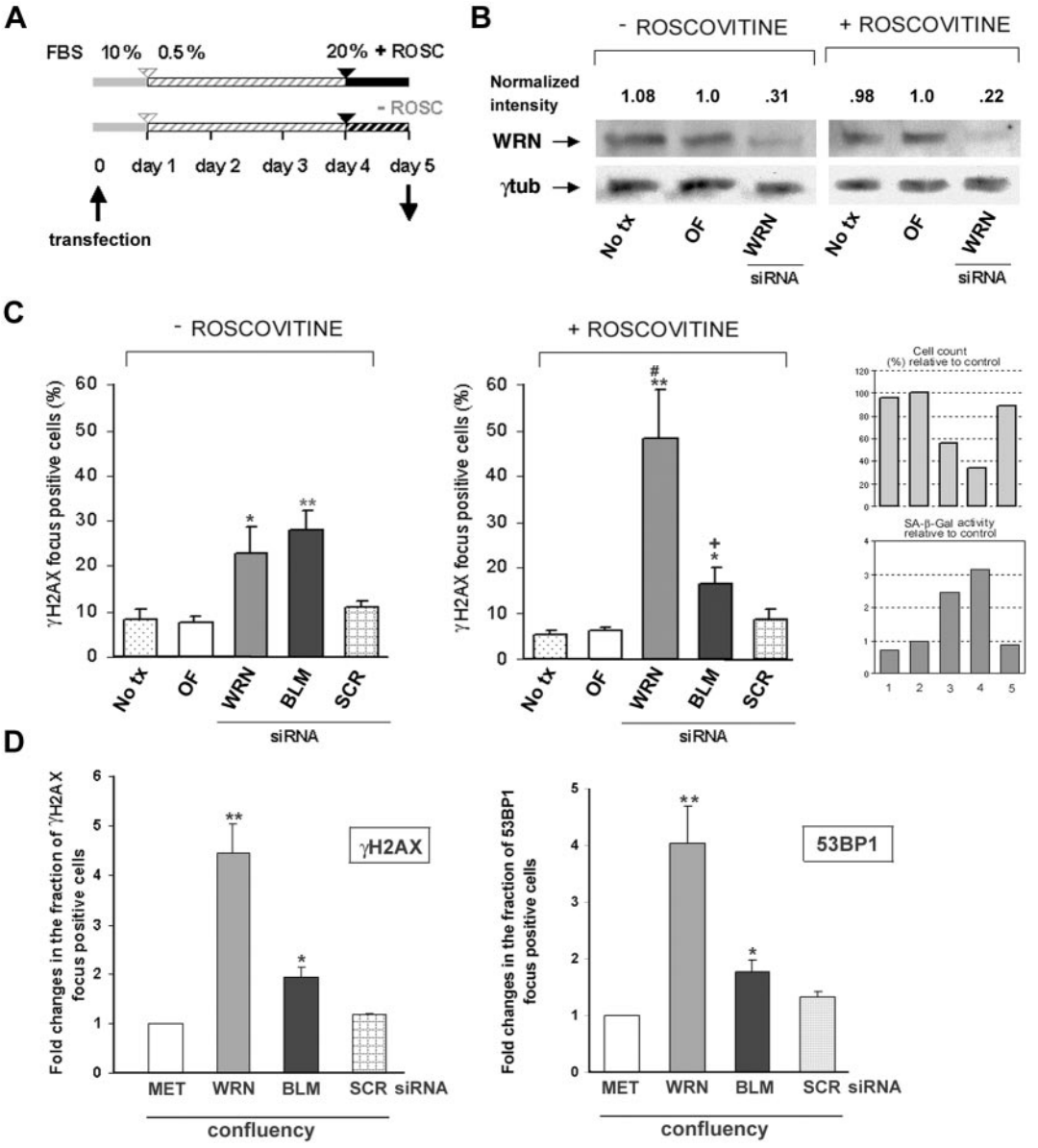

FIG. 5. Acute knockdown of WRN, but not BLM, results in augmented DNA damage in nonreplicating cells arrested in G_1 phase. (A) Experimental time line. After the various siRNA transfections the cells were synchronized with 0.5% serum for 72 h and then further cultured in 20% serum in the absence or presence of 20 μM roscovitine for 24 h. (B) Quantitative immunoblot analysis of WRN protein expression in WI-38 cells synchronized by roscovitine, as shown in the experimental schedule. At day 5 posttransfection total cell lysates were harvested and analyzed by Western blotting for WRN and γ-tubulin expression. The normalized intensities of the WRN signal are indicated. (C) Quantification of γH2AX formation. Histograms show the percentage of focus-positive cells after various siRNA transfections as indicated. Minimum 250 intact nuclei were screened per condition in at least three independent biological experiments. Error bars represent the SEM. The levels of statistically significant differences are indicated as follows: *, $P < 0.05$; and **, $P < 0.01$ (compared to the respective Oligofectamine [OF] controls). Statistically significant differences between G_1-arrested or replicating WRN-depleted cells (#, $P < 0.05$) and BLM-depleted cells (+, $P < 0.02$) are indicated. The inset displays the normalized percentage of cell number and fold changes in SA-β-Gal-positive cells synchronized by roscovitine, the values represent the average of two independent experiments. Columns: 1, no treatment; 2, Oligofectamine (OF); 3, WRN siRNA; 4, BLM siRNA; 5, SCR siRNA. (D) Effect of cell cycle arrest by confluence on the formation of γH2AX and 53BP1 foci formation. To arrest the cells at confluence, the initial plating was performed at high density (~80% confluence) and Metafectene was used to introduce siRNA to the cells. For comparison, fold changes in the fraction of 53BP1- positive cells were calculated by using the transfection reagent treated cells as baseline. MET, Metafectene. The SEMs of three experiments are shown; **, $P < 0.05$.

replication or at sites of DNA repair in the absence of cell division. Therefore, we studied the accumulation of γH2AX foci under conditions of low-oxygen tension in asynchronous and G_1 cell cycle-arrested cells (Fig. 6A). Although replicating cells maintained strictly at 3% oxygen tension and transfected with BLM siRNA alone or in combination with WRN siRNA continued to accumulate γH2AX foci, low-oxygen tension prevented the induction of γH2AX foci in replicating WRN-de-

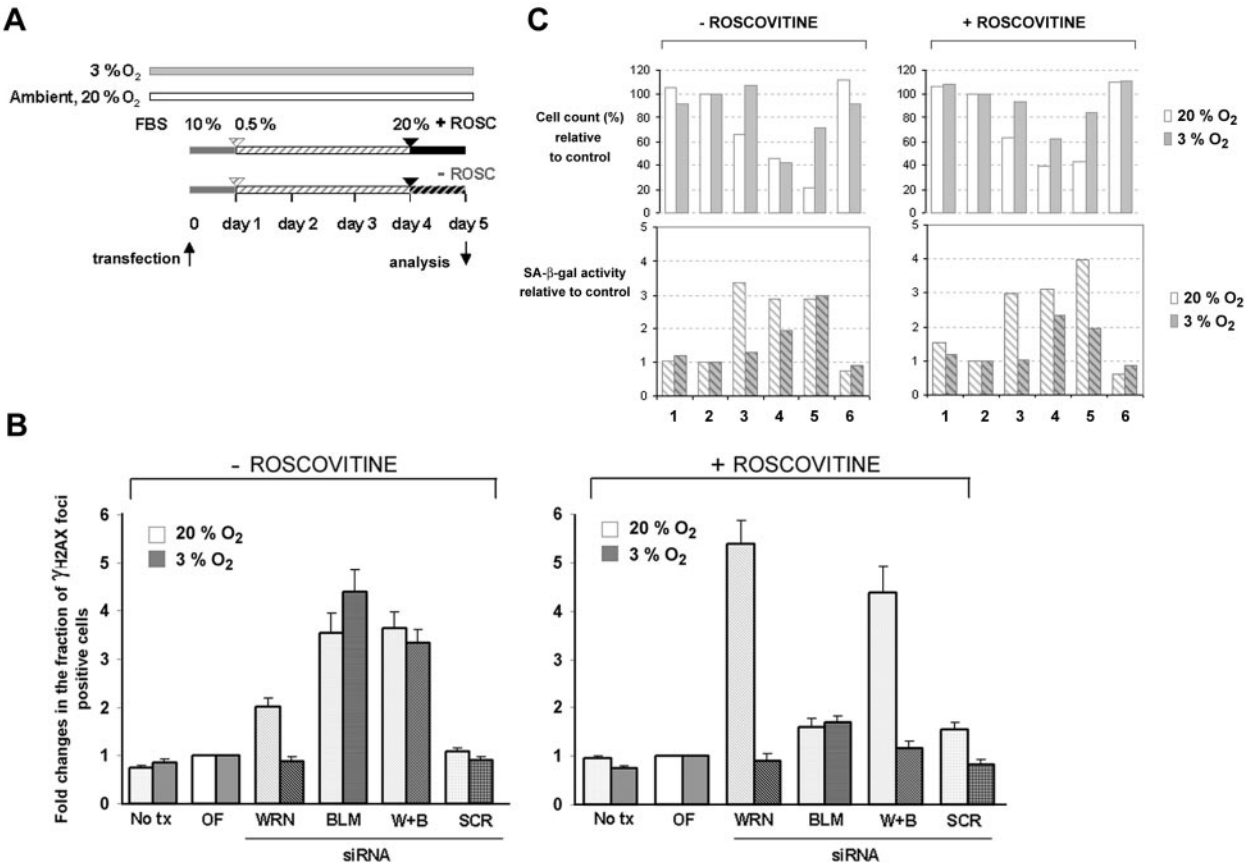

FIG. 6. Lowering oxygen tension preferentially suppresses DNA damage in WRN depleted cells. (A) Experimental schedule. WI-38 primary fibroblasts (PDL 24 to 26) were plated at ~30% confluence and cultured in 20% or 3% oxygen throughout, as indicated. siRNA transfection was performed within 24 h after plating, followed by cell cycle synchronization using roscovitine as described at the legend of Fig. 4. (B) Quantitation of γH2AX formation. Histograms show the fold changes in the fraction of focus-positive cells, normalized to their respective mock-transfected (Oligofectamine [OF]) controls, after various siRNA transfections. The cells were maintained in 20% (light bars) or strictly 3% oxygen tension (dark bars) and synchronized with roscovitine as indicated. The error bars show the SEMs of three independent experiments. (C) Cell growth and SA-β-Gal activity of fibroblasts grown either in 20% or 3% oxygen and synchronized by roscovitine. The values are normalized to mock transfection. The bars represent the average from at least two independent experimental series. Minimum 250 nuclei were screened per individual datum point in each experiment. Columns: 1, no treatment; 2, Oligofectamine (OF); 3, WRN siRNA; 4, BLM siRNA; 5, WRN + BLM siRNAs; 6, SCR siRNA.

pleted cells (Fig. 6B, left panel). In addition, 3% oxygen fully suppressed the augmented foci formation seen in WRN- or simultaneous WRN- and BLM-depleted cells synchronized with roscovitine (Fig. 6B, right panel). Although the fibroblasts grew faster in low oxygen as shown previously (9), the siRNA-mediated inhibition of WRN and BLM mRNA expression and the extent of protein depletion were comparable to that at ambient O_2 (84% decrease of WRN protein expression by immunoblotting and 54% decrease of BLM mRNA expression by real-time RT-PCR). Low-oxygen tension also prevented the decreased cellular growth and increased SA-β-Gal activity that were seen at ambient oxygen after WRN RNAi (Fig. 6C).

To confirm that withdrawal of WRN from cells renders them more sensitive to oxidative damage, we examined the sensitivity of normal fibroblasts, maintained in 20 or 3% oxygen, to form γH2AX foci in response to various doses of hydrogen peroxide treatment. In comparison to cells cultured in ambient oxygen, normal cells maintained at 3% oxygen were more resistant to H_2O_2, but their potential to mount a γH2AX response was unaltered by the low-oxygen condition (Fig. 7A). Cells maintained at 3% oxygen were then transfected with WRN or control siRNAs. At 96 h posttransfection the cells were treated with a 45-min pulse of 75 μM H_2O_2 in serum-free medium, a concentration previously determined to yield γH2AX foci in the majority of treated cells. The cells were either fixed immediately after the pulse or, after a medium change, were allowed to recover for the indicated period of time at 3% O_2 and then evaluated for the presence of DNA damage foci. As shown in Fig. 7B, cells transfected by WRN siRNA showed a modestly higher level of foci immediately after exposure to hydrogen peroxide. However, by 6 and 28 h after the H_2O_2 treatment, the number of foci in the WRN siRNA transfected cells was severalfold higher than in control cells. Similar results were also obtained with cells synchronized with roscovitine to prevent cell replication (unpublished data). The increased number and persistence of the oxidative damage induced by H_2O_2 in WRN-depleted cells cultured at 3% oxygen indicate a delay or defect in the rate of DNA repair in these cells.

An additional confirmation of the role of O_2 in producing

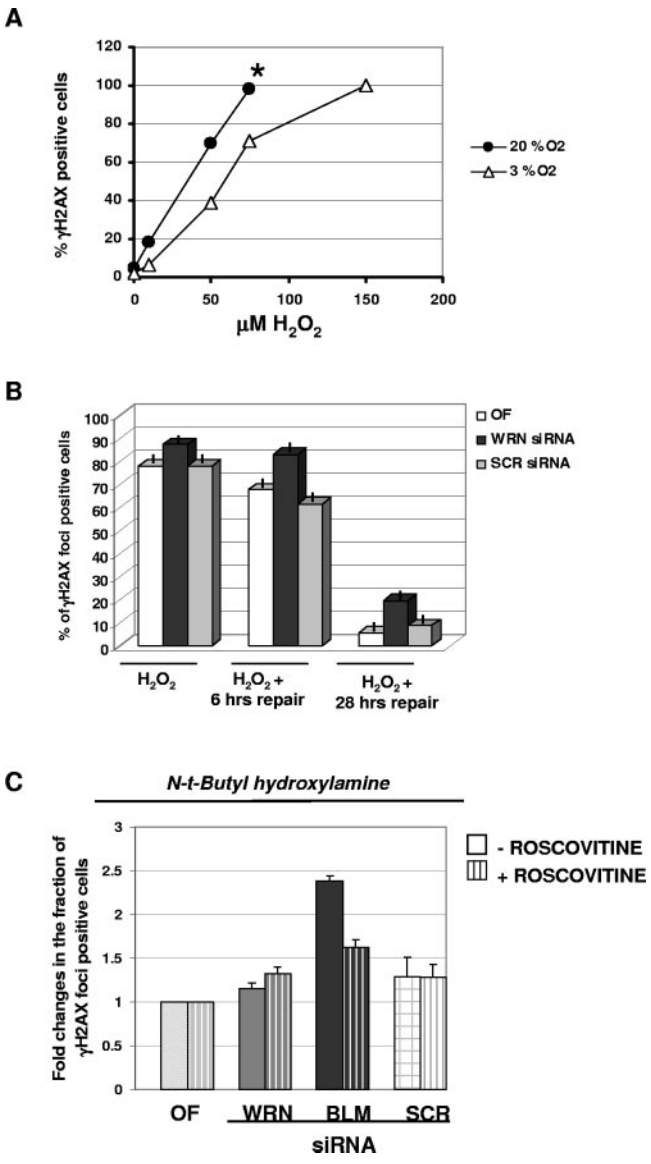

FIG. 7. Increased sensitivity of WRN-depleted cells to different types of oxidative damage. (A) Sensitivity of normal fibroblasts, maintained in ambient (20%) or 3% oxygen, to form γH2AX foci in response to various doses of hydrogen peroxide treatment. Asynchronous WI-38 cells were cultured under 20% and 3% oxygen and treated for 45 min with the indicated doses of H_2O_2 in serum free-medium, followed by fixation and immunofluorescence analysis. The asterisk indicates a mild to moderate amount of cell death in 20% oxygen, which became predominant at a 150 μM H_2O_2 dose. (B) Prolonged presence of DNA damage foci induced by acute hydrogen peroxide treatment in WRN-depleted cells. WI-38 cells were cultured under 3% oxygen. At 96 h after siRNA transfection, the cells were treated for 45 min with 75 μM H_2O_2 in serum free-medium then either processed immediately for immunofluorescence analysis or, after medium change, allowed to recover at 3% oxygen for various amounts of time, as indicated. Bars indicate the percentage of γH2AX focus-positive cells. Error bars show the SEMs of three experiments. (C) The antioxidant NtBHA protects WRN-depleted cells to develop DNA damage foci at ambient oxygen. The cells were subcultured at 20% oxygen in the presence of 100 μM NtBHA for 2 weeks and then transfected with the various siRNAs and synchronized by roscovitine as described to Fig. 5. The error bars show the SEMs of three experiments.

DNA damage in WRN siRNA-treated cells was obtained by growing the cells at ambient oxygen for 2 weeks in the presence of the anti-oxidant NtBHA, a chemical that scavenges endogenous hydroxyl radicals (1, 2), before introduction of siRNA. Cells cultured in medium containing NtBHA and treated with WRN siRNA showed only a minimal increase in the number of DNA damage foci compared to control cells (Fig. 7C). This was true both in replicating cells without roscovitine treatment and in cells arrested with roscovitine (Fig. 7C). BLM-depleted asynchronous or synchronously replicating cells cultivated in the presence of NtBHA continued to show elevated numbers of DNA damage foci (Fig. 7C, minus roscovitine). As in the previous experiments, roscovitine-arrested BLM-depleted cells had substantially reduced number of γH2AX foci (Fig. 7C, plus roscovitine). The mechanism of DNA damage focus formation remained intact in normal primary fibroblasts of these experiments. In response to the DNA cross-linking agent mitomycin C, the cells showed a similar degree of DNA damage focus formation whether they were subcultured under standard condition in 20% oxygen, in the presence of NtBHA at 20% oxygen or maintained in 3% oxygen (data not shown).

Overexpression of TRF2 prevents WRN RNAi-mediated DNA damage response in nonreplicating primary fibroblasts. WRN and BLM have both been implicated in telomere maintenance by the ALT mechanism in cells that lack telomerase (38, 39). Forced telomerase expression immortalizes WS cells and decreases the sensitivity of these cells to 4-NQO (26). TRF2 protein binds to telomere repeats and has been implicated in the protection of telomere ends and the formation of T-loops at telomeres (for a review, see reference 51). Modulation of the level of TRF2 has been used to study the effects of uncapped telomere ends in vivo (29). TRF2 can also bind to and stimulate WRN and BLM helicases in vitro (39). Furthermore, components of the cellular DNA damage response machinery respond to dysfunctional telomeres that occur in the absence of functional TRF2 (12, 54). Therefore, we sought to determine whether enforced expression of TRF2 would modify the DNA damage response induced by depletion of WRN and BLM helicases in G_1-arrested primary human fibroblasts at ambient and physiological low oxygen. Full-length TRF2 and a dominant-negative form of TRF2 (DN-TRF2) were transfected to primary fibroblasts, followed by transfection of various siRNAs. Quantitative immunoblot analysis verified the TRF2 and DN-TRF2 overexpression. Furthermore, WRN RNAi failed to significantly alter the expression of TRF2 and that TRF2 and DN-TRF2 overexpression did not change WRN protein levels (Fig. 8A). The extent of DNA damage was monitored by quantifying γH2AX 5 days after sequential transfection of full-length TRF2 or DN-TRF2 cDNAs and various siRNAs (Fig. 8B and C). In asynchronously (Fig. 8B) and synchronously replicating cells (Fig. 8C, left panel), the WRN RNAi-induced DNA damage response was largely prevented by overexpression of TRF2. The TRF2 rescue of the WRN knockdown cells was not mediated by alteration of WRN levels (Fig. 8A). Strikingly, cells transfected with the full-length TRF2 expressing construct prior to WRN RNAi followed by roscovitine-synchronization and G_1 arrest showed no induction of DNA damage foci (Fig. 8C, right panel). BLM RNAi-induced γH2AX focus formation was essentially unaf-

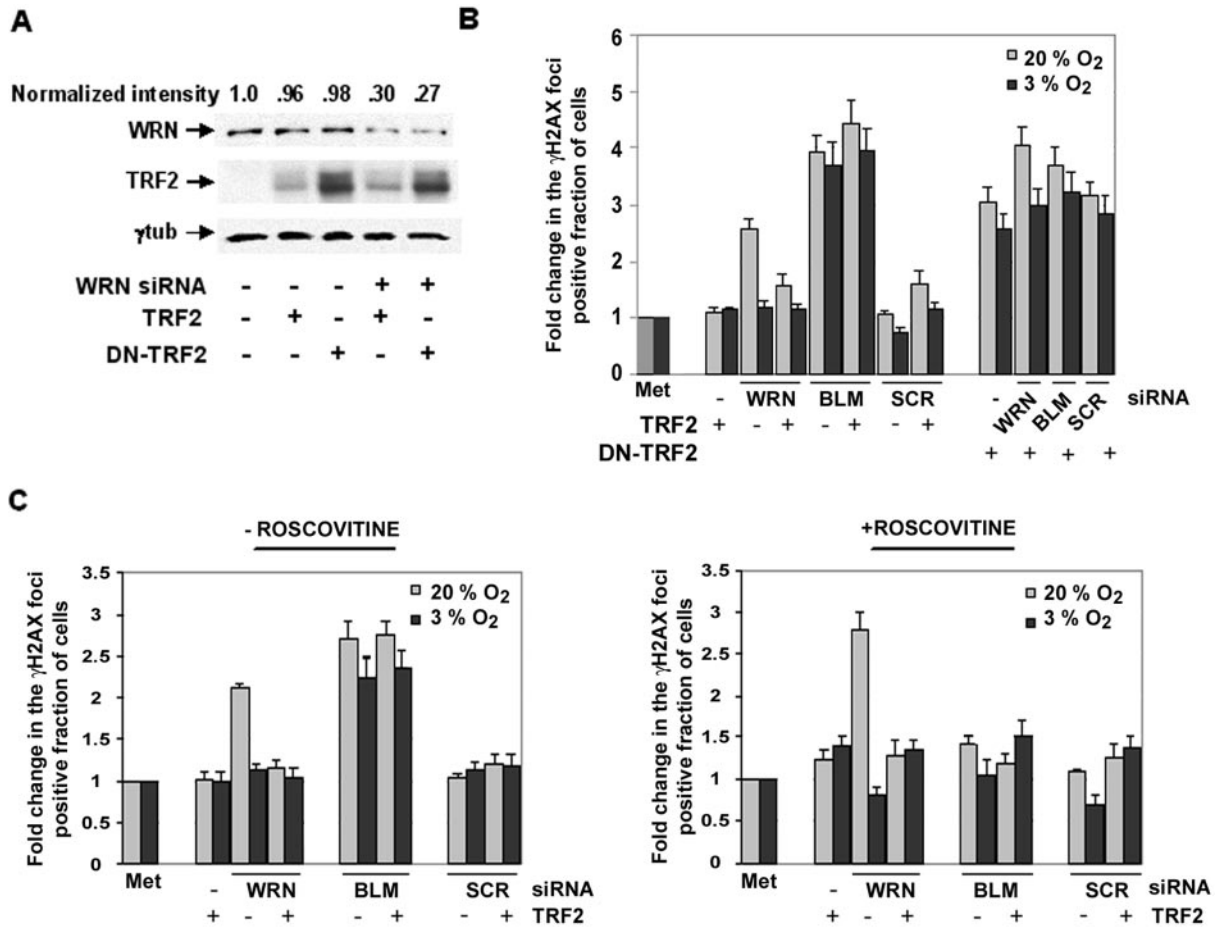

FIG. 8. Effect of TRF2 on WRN and BLM RNAi-induced γH2AX focus formation in G_1-arrested primary fibroblasts. (A) Immunoblot analysis of WRN and TRF2 protein expression 4 days after transfection of full-length TRF2 or DN-TRF2 and WRN siRNA. Radioimmunoprecipitation assay lysates were analyzed by Western blotting. The quantified intensities of WRN immunoreactivity is shown normalized to mock-transfected cells and γ-tubulin as loading control. (B) Comparison of the effects of TRF2 and DN-TRF2 in asynchronous cell population. Cells grown either at ambient (20%) or 3% oxygen were sequentially transfected first with full-length TRF2 or its dominant-negative mutant form, DN-TRF2, followed by transfection of various siRNAs as described above. (C) Effect of TRF2 overexpression in cells synchronized by roscovitine as described under Fig. 5. Minimum 250 cells were analyzed at each condition. The error bars represent the SEMs of three experiments.

fected by TRF2 either in replicating or G_1-arrested cells. The effect of TRF2 overexpression appears largely independent of the oxygen tension (compare light and dark shaded bars in each condition).

These data again show a dissociation of WRN and BLM functions in vivo in untransformed human cells and raise the possibility that, particularly in nonreplicating cells, WRN may have direct effects on the telomeres or TRF2 may play a specific role in repair of the types of DNA lesions that occur in these cells. As has been reported (12, 54), transfecting the cells with the dominant-negative form of TRF2 produced an increased number of foci, even at 3% O_2, and the number of foci was not significantly altered by either WRN or BLM siRNA (Fig. 8B). This is consistent with the original report that this form of TRF2 induced foci by destabilizing telomere capping, an event that need not be affected by oxygen toxicity.

DISCUSSION

To understand the relationship between the molecular abnormality in Werner syndrome and the consequent organismal phenotype, we sought to identify cellular processes that are vulnerable to WRN deficiency but not to deficiency of BLM, the related helicase implicated in Bloom syndrome. Nonreplicating cells were particularly prone to develop a DNA damage response after WRN loss. In contrast, the effects of BLM loss were much more prominent in replicating cells. Unlike the cellular response to BLM RNAi, the response to WRN RNAi was inhibited by enforced expression of the protein TRF2 and was specifically dependent on the presence of oxidative stress. This was evidenced by the normal growth of WRN-depleted cells at physiologic levels of oxygen, by the improvement in their growth and decrease in the number of DNA damage foci when the cells were grown at 20% oxygen in the presence of an antioxidant, and by the increased number and delayed clearance of DNA damage foci in WRN-depleted cells challenged by moderate concentrations of H_2O_2.

Presumably, γH2AX foci would not be apparent if DNA damage occurred but was rapidly repaired or if the presence of the RNAi-targeted protein was necessary for their formation.

However, in the experiments using roscovitine synchronization and low oxygen, in which foci were not prominent in BLM or WRN knockdown cells, the lack of foci was not due to a general requirement for the missing protein to form foci since simultaneous depletion of WRN and BLM still produced these foci in replicating cells (Fig. 6B, left panel). Furthermore, normal fibroblasts developed a similar degree of foci formation in response to mitomycin C, whether they were subcultured under standard condition, in the presence of NtBHA at 20% oxygen, or maintained in 3% oxygen. Our conclusion is that WRN, differently from BLM, plays a specific role in preventing or repairing DNA lesions resulting from chronic, oxidative stress with particular impact on slowly replicating cells. In contrast, BLM is specifically needed to resolve DNA lesions that arise during DNA replication.

Oxidative damage to DNA is known to cause a number of lesions, many of which involve damage of single bases (11, 21). A major mechanism for the repair of these lesions in both resting and replicating cells is base excision repair (BER). Diminished poly ADP-ribosylation of proteins has been observed in WRN-deficient cells (55). This decrease in protein modification has been suggested to impair the BER pathway, and this in turn could sensitize the cells to oxygen toxicity. In vitro functional interaction of WRN with DNA polymerase β, a significant enzyme of BER, has also been shown (24). The mechanisms by which single-stranded DNA lesions and repair can activate formation of DNA damage foci in nonreplicating cells is not entirely clear. DSBs may be caused directly by oxidative damage. It is conceivable that DNA nicking repair processes such as DNA glycosidase and apurinic nuclease action might be directed to the complementary DNA strand in the presence of a single-stranded DNA lesion that cannot be efficiently repaired. Alternatively, the DNA damage foci in the WRN knockdown cells may be a result of other lesions than DSBs. More precise knowledge of the types and mechanisms of production of lesions accumulating in Werner cells is badly needed.

The majority of studies of WRN cells have used cells from individuals who congenitally lacked WRN protein and therefore had undergone a prolonged selection for adaptation to WRN deficiency. Recently, WRN was knocked down in normal fibroblasts by transfection with a retrovirus expressing a WRN siRNA and a puromycin resistance gene (57). These cells, studied after selection in puromycin, showed a slow growth in ambient oxygen, and this could be further reduced by H_2O_2 treatment. The effects of physiological oxygen concentration or antioxidant were not studied, and differences in protocols prevent an exact comparison of this slow growth with the growth arrest we observed within days in cells after WRN siRNA transfection.

Acute silencing of endogenous WRN and BLM expression in asynchronous cells led to development of stigmata of cellular senescence. Consistent with several other reports (5, 52, 57), the p53 response in cells depleted of WRN was weak. However, the presence of Rb protein could be sufficient to induce senescence even when p53 function was abrogated. The stalled growth and prominent senescence produced by acute knockdown of WRN in primary fibroblasts contrasts with the growth features of cells derived from Werner patients. Primary cells from Werner patients, although growing poorly, have been passaged in culture and can be immortalized with SV40 virus, Epstein-Barr virus, or telomerase (10, 27). Werner patients also develop normally through childhood. A likely explanation for these differences is that cells derived from Werner patients have adapted in some way to the absence of WRN. A striking example of differences between cellular effects of acute compared to chronic absence of a protein has been recently described for the Rb cell cycle regulator (45). Such reports reinforce the principle that acute perturbations are necessary to assess the normal role of a protein.

Although the BLM and WRN helicases have similar specificities and presumably each has a role in several processes, they appear to function in different phases of the cell cycle. Our results are consistent with the reports of cell-cycle-regulated production of BLM mRNA with mRNA levels peaking at S and G_2 and an increased sensitivity of cells from Bloom syndrome patient to DNA damage in S, but not G_1 phase, suggesting a pivotal role of BLM in response of replicational stress (4, 13, 14, 17). Mechanisms activated during replication might actually repair the lesions that accumulate in G_1 in WRN-deficient cells. This could account for the relatively normal appearance of rapidly replicating cells (such as those in the bone marrow and intestinal epithelium) in Werner syndrome and in normal aging. Defects in DNA replication and development of chromosomal abnormalities in Werner cells might be a secondary consequence of failure to repair DNA lesions accumulated during prolonged G_1.

TRF2 was detected originally as a telomere-binding protein, and overexpression of this protein was shown to have a protective effect on critically short telomeres in primary fibroblasts (29, 51). TRF2 strikingly prevented the development of γH2AX foci in nonreplicating cells depleted of WRN but not in cells depleted of BLM. In principle, dynamic uncapping of telomeres could be synergistic with DNA damage stimuli arising from lesions elsewhere in the chromosome and augment the formation of foci. The lack of effect of TRF2 on the BLM RNAi-induced damage foci argues somewhat against this and shows that overproduction of TRF2 does not itself block mechanisms of foci formation. It is possible that WRN could normally play a role in maintenance of the capped structure or DNA repair at telomeres in nondividing cells. Another possibility is that TRF2 could directly or indirectly mediate G_0/G_1 repair of DNA lesions elsewhere than at the telomere. Importantly, after the present manuscript was submitted for publication, a report appeared showing that TRF2 rapidly accumulated at the site of induced DNA breaks, suggesting a nontelomeric role for TRF2 in repair of DNA damage (6). Also, after the present study was completed, papers were published showing that late-generation telomerase and WRN double-knockout mice developed manifestations resembling Werner syndrome (8, 16). Notably, telomere DNA sequences may be particularly sensitive to oxygen damage and the role of oxidative damage in producing telomere damage and shortening has been extensively discussed (58). In this context, it will be important to determine whether the DNA damage foci in WRN-depleted cells are concentrated at or near telomeres.

In metazoan models of aging most pathology occurs in organs made up of slowly dividing or nondividing cells. Our data suggest that manifestations of Werner syndrome might be attributable to defects in repairing oxidative DNA damage that

occur in slowly replicating cells. We also suggest that over time lesions would accumulate that impair the ability of precursor cells such as mesenchymal stem cells from replicating and replenishing tissues such as adipose tissue and bone osteoblasts. Lack of adipose tissue would result in elevated fatty acid levels in serum and induce a lipodystrophy such as diabetes, and osteoblast deficiency could account for the osteoporosis. Our observations attest to the concept, supported by recent studies with mouse cells (28, 40), that impaired DNA repair and genomic instability, driven by oxidative damage, may underlie normal human aging.

ACKNOWLEDGMENTS

We are grateful for the 53BP1 antibody and the full-length TRF2 and DN-TRF2 cDNAs provided by T. Halazonetis and T. de Lange, respectively. We thank S. Potluri for excellent help in the experimental work.

A.M.S. is supported by a Mentored Clinical Scientist Award (KO8-AG01053) from the NIA. S.M.W. was awarded by the Ellison Medical Foundation Senior Scholar Program in Aging.

REFERENCES

1. **Atamna, H., A. Paler-Martinez, and B. N. Ames.** 2000. *N-t*-butyl hydroxylamine, a hydrolysis product of alpha-phenyl-*N-t*-butyl nitrone, is more potent in delaying senescence in human lung fibroblasts. J. Biol. Chem. **275:**6741–6748.
2. **Atamna, H., C. Robinson, R. Ingersoll, H. Elliott, and B. N. Ames.** 2001. N-t-Butyl hydroxylamine is an antioxidant that reverses age-related changes in mitochondria in vivo and in vitro. FASEB J. **15:**2196–2204.
3. **Beckman, K. B., and B. N. Ames.** 1998. The free radical theory of aging matures. Physiol. Rev. **78:**547–581.
4. **Bischof, O., S. H. Kim, J. Irving, S. Beresten, N. A. Ellis, and J. Campisi.** 2001. Regulation and localization of the Bloom syndrome protein in response to DNA damage. J. Cell Biol. **153:**367–380.
5. **Blander, G., N. Zalle, J. F. Leal, R. L. Bar-Or, C. E. Yu, and M. Oren.** 2000. The Werner syndrome protein contributes to induction of p53 by DNA damage. FASEB J. **14:**2138–2140.
6. **Bradshaw, P. S., D. J. Stavropoulos, and M. S. Meyn.** 2005. Human telomeric protein TRF2 associates with genomic double-strand breaks as an early response to DNA damage. Nat. Genet. **37:**193–197.
7. **Celeste, A., S. Petersen, P. J. Romanienko, O. Fernandez-Capetillo, H. T. Chen, O. A. Sedelnikova, B. Reina-San-Martin, V. Coppola, E. Meffre, M. J. Difilippantonio, C. Redon, D. R. Pilch, A. Olaru, M. Eckhaus, R. D. Camerini-Otero, L. Tessarollo, F. Livak, K. Manova, W. M. Bonner, M. C. Nussenzweig, and A. Nussenzweig.** 2002. Genomic instability in mice lacking histone H2AX. Science **296:**922–927.
8. **Chang, S., A. S. Multani, N. G. Cabrera, M. L. Naylor, P. Laud, D. Lombard, S. Pathak, L. Guarente, and R. A. DePinho.** 2004. Essential role of limiting telomeres in the pathogenesis of Werner syndrome. Nat. Genet. **36:**877–882.
9. **Chen, Q., A. Fischer, J. D. Reagan, L. J. Yan, and B. N. Ames.** 1995. Oxidative DNA damage and senescence of human diploid fibroblast cells. Proc. Natl. Acad. Sci. USA **92:**4337–4341.
10. **Choi, D., P. S. Whittier, J. Oshima, and W. D. Funk.** 2001. Telomerase expression prevents replicative senescence but does not fully reset mRNA expression patterns in Werner syndrome cell strains. FASEB J. **15:**1014–1020.
11. **Cooke, M. S., M. D. Evans, M. Dizdaroglu, and J. Lunec.** 2003. Oxidative DNA damage: mechanisms, mutation, and disease. FASEB J. **17:**1195–1214.
12. **d'Adda di Fagagna, F., P. M. Reaper, L. Clay-Farrace, H. Fiegler, P. Carr, T. Von Zglinicki, G. Saretzki, N. P. Carter, and S. P. Jackson.** 2003. A DNA damage checkpoint response in telomere-initiated senescence. Nature **426:**194–198.
13. **Davalos, A. R., and J. Campisi.** 2003. Bloom syndrome cells undergo p53-dependent apoptosis and delayed assembly of BRCA1 and NBS1 repair complexes at stalled replication forks. J. Cell Biol. **162:**1197–1209.
14. **Davies, S. L., P. S. North, A. Dart, N. D. Lakin, and I. D. Hickson.** 2004. Phosphorylation of the Bloom's syndrome helicase and its role in recovery from S-phase arrest. Mol. Cell. Biol. **24:**1279–1291.
15. **Dimri, G. P., X. Lee, G. Basile, M. Acosta, G. Scott, C. Roskelley, E. E. Medrano, M. Linskens, I. Rubelj, O. Pereira-Smith, et al.** 1995. A biomarker that identifies senescent human cells in culture and in aging skin in vivo. Proc. Natl. Acad. Sci. USA **92:**9363–9367.
16. **Du, X., J. Shen, N. Kugan, E. E. Furth, D. B. Lombard, C. Cheung, S. Pak, G. Luo, R. J. Pignolo, R. A. DePinho, L. Guarente, and F. B. Johnson.** 2004. Telomere shortening exposes functions for the mouse Werner and Bloom syndrome genes. Mol. Cell. Biol. **24:**8437–8446.
17. **Dutertre, S., M. Ababou, R. Onclercq, J. Delic, B. Chatton, C. Jaulin, and M. Amor-Gueret.** 2000. Cell cycle regulation of the endogenous wild type Bloom's syndrome DNA helicase. Oncogene **19:**2731–2738.
18. **Elbashir, S. M., J. Harborth, K. Weber, and T. Tuschl.** 2002. Analysis of gene function in somatic mammalian cells using small interfering RNAs. Methods **26:**199–213.
19. **Ellis, N. A., J. Groden, T. Z. Ye, J. Straughen, D. J. Lennon, S. Ciocci, M. Proytcheva, and J. German.** 1995. The Bloom's syndrome gene product is homologous to RecQ helicases. Cell **83:**655–666.
20. **Epstein, C. J., and A. G. Motulsky.** 1996. Werner syndrome: entering the helicase era. Bioessays **18:**1025–1027.
21. **Evans, M. D., M. Dizdaroglu, and M. S. Cooke.** 2004. Oxidative DNA damage and disease: induction, repair and significance. Mutat. Res. **567:**1–61.
22. **Fernandez-Capetillo, O., A. Lee, M. Nussenzweig, and A. Nussenzweig.** 2004. H2AX: the histone guardian of the genome. DNA Repair **3:**959–967.
23. **Fukuchi, K., G. M. Martin, and R. J. Monnat, Jr.** 1989 Mutator phenotype of Werner syndrome is characterized by extensive deletions. Proc. Natl. Acad. Sci. USA **86:**5893–5897.
24. **Harrigan, J. A., P. L. Opresko, C. von Kobbe, P. S. Kedar, R. Prasad, S. H. Wilson, and V. A. Bohr.** 2003. The Werner syndrome protein stimulates DNA polymerase beta strand displacement synthesis via its helicase activity. J. Biol. Chem. **278:**22686–22695.
25. **Hickson, I. D.** 2003. RecQ helicases: caretakers of the genome. Nat. Rev. Cancer **3:**169–178.
26. **Hisama, F. M., Y. H. Chen, M. S. Meyn, J. Oshima, and S. M. Weissman.** 2000. WRN or telomerase constructs reverse 4-nitroquinoline 1-oxide sensitivity in transformed Werner syndrome fibroblasts. Cancer Res. **60:**2372–2376.
27. **Huschtscha, L. I., K. V. Thompson, and R. Holliday.** 1986. The susceptibility of Werner's syndrome and other human skin fibroblasts to SV40-induced transformation and immortalization. Proc. R. Soc. Lond. B Biol. Sci. **229:**1–12.
28. **Karanjawala, Z. E., N. Murphy, D. R. Hinton, C. L. Hsieh, and M. R. Lieber.** 2002. Oxygen metabolism causes chromosome breaks and is associated with the neuronal apoptosis observed in DNA double-strand break repair mutants. Curr. Biol. **12:**397–402.
29. **Karlseder, J., A. Smogorzewska, and T. de Lange.** 2002. Senescence induced by altered telomere state, not telomere loss. Science **295:**2446–2449.
30. **Kitao, S., A. Shimamoto, M. Goto, R. W. Miller, W. A. Smithson, N. M. Lindor, and Y. Furuichi.** 1999. Mutations in RECQL4 cause a subset of cases of Rothmund-Thomson syndrome. Nat. Genet. **22:**82–84.
31. **Lombard, D. B., C. Beard, B. Johnson, R. A. Marciniak, J. Dausman, R. Bronson, J. E. Buhlmann, R. Lipman, R. Curry, A. Sharpe, R. Jaenisch, and L. Guarente.** 2000. Mutations in the WRN gene in mice accelerate mortality in a p53-null background. Mol. Cell. Biol. **20:**3286–3291.
32. **Martin, G. M., and J. Oshima.** 2000. Lessons from human progeroid syndromes. Nature **408:**263–266.
33. **Martin, G. M., J. Oshima, M. D. Gray, and M. Poot.** 1999. What geriatricians should know about the Werner syndrome. J. Am. Geriatr. Soc. **47:**1136–1144.
34. **Mochan, T. A., M. Venere, R. A. DiTullio, Jr., and T. D. Halazonetis.** 2004. 53BP1, an activator of ATM in response to DNA damage. DNA Repair **3:**945–952.
35. **Monnat, R. J., Jr., and Y. Saintigny.** 2004. Werner syndrome protein-unwinding function to explain disease. Sci. Aging Knowledge Environ. **13:**1–10.
36. **Neff, N. F., N. A. Ellis, T. Z. Ye, J. Noonan, K. Huang, M. Sanz, and M. Proytcheva.** 1999. The DNA helicase activity of BLM is necessary for the correction of the genomic instability of bloom syndrome cells. Mol. Biol. Cell **10:**665–676.
37. **Opresko, P. L., W. H. Cheng, and V. A. Bohr.** 2004. Junction of RecQ helicase biochemistry and human disease. J. Biol. Chem. **279:**18099–18102.
38. **Opresko, P. L., M. Otterlei, J. Graakjaer, P. Bruheim, L. Dawut, S. Kolvraa, A. May, M. M. Seidman, and V. A. Bohr.** 2004. The Werner syndrome helicase and exonuclease cooperate to resolve telomeric D loops in a manner regulated by TRF1 and TRF2. Mol. Cell **14:**763–774.
39. **Opresko, P. L., C. von Kobbe, J. P. Laine, J. Harrigan, I. D. Hickson, and V. A. Bohr.** 2002. Telomere-binding protein TRF2 binds to and stimulates the Werner and Bloom syndrome helicases. J. Biol. Chem. **277:**41110–41119.
40. **Parrinello, S., E. Samper, A. Krtolica, J. Goldstein, S. Melov, and J. Campisi.** 2003. Oxygen sensitivity severely limits the replicative lifespan of murine fibroblasts. Nat. Cell Biol. **5:**741–747.
41. **Reynolds, T. Y., S. Rockwell, and P. M. Glazer.** 1996. Genetic instability induced by the tumor microenvironment. Cancer Res **56:**5754–5757.
42. **Rodriguez-Lopez, A. M., D. A. Jackson, F. Iborra, and L. S. Cox.** 2002. Asymmetry of DNA replication fork progression in Werner's syndrome. Aging Cell **1:**30–39.
43. **Rogakou, E. P., C. Boon, C. Redon, and W. M. Bonner.** 1999. Megabase chromatin domains involved in DNA double-strand breaks in vivo. J. Cell Biol. **146:**905–916.
44. **Rothkamm, K., and M. Lobrich.** 2003. Evidence for a lack of DNA double-

strand break repair in human cells exposed to very low x-ray doses. Proc. Natl. Acad. Sci. USA **100:**5057–5062.
45. **Sage, J., A. L. Miller, P. A. Perez-Mancera, J. M. Wysocki, and T. Jacks.** 2003. Acute mutation of retinoblastoma gene function is sufficient for cell cycle re-entry. Nature **424:**223–228.
46. **Salk, D.** 1982. Werner's syndrome: a review of recent research with an analysis of connective tissue metabolism, growth control of cultured cells, and chromosomal aberrations. Hum. Genet. **62:**1–5.
47. **Salk, D., K. Au, H. Hoehn, M. R. Stenchever, and G. M. Martin.** 1981. Evidence of clonal attenuation, clonal succession, and clonal expansion in mass cultures of aging Werner's syndrome skin fibroblasts. Cytogenet. Cell Genet. **30:**108–117.
48. **Schultz, L. B., N. H. Chehab, A. Malikzay, and T. D. Halazonetis.** 2000. p53 binding protein 1 (53BP1) is an early participant in the cellular response to DNA double-strand breaks. J. Cell Biol. **151:**1381–1390.
49. **Senderowicz, A. M.** 2003. Small-molecule cyclin-dependent kinase modulators. Oncogene **22:**6609–6620.
50. **Siitonen, H. A., O. Kopra, H. Kaariainen, H. Haravuori, R. M. Winter, A. M. Saamanen, L. Peltonen, and M. Kestila.** 2003. Molecular defect of RAPADILINO syndrome expands the phenotype spectrum of RECQL diseases. Hum. Mol. Genet. **12:**2837–2844.
51. **Smogorzewska, A., and T. de Lange.** 2004. Regulation of telomerase by telomeric proteins. Annu. Rev. Biochem. **73:**177–208.
52. **Spillare, E. A., A. I. Robles, X. W. Wang, J. C. Shen, C. E. Yu, G. D. Schellenberg, and C. C. Harris.** 1999. p53-mediated apoptosis is attenuated in Werner syndrome cells. Genes Dev. **13:**1355–1360.
53. **Szekely, A. M., Y. H. Chen, C. Zhang, J. Oshima, and S. M. Weissman.** 2000. Werner protein recruits DNA polymerase delta to the nucleolus. Proc. Natl. Acad. Sci. USA **97:**11365–11370.
54. **Takai, H., A. Smogorzewska, and T. de Lange.** 2003. DNA damage foci at dysfunctional telomeres. Curr. Biol. **13:**1549–1556.
55. **von Kobbe, C., J. A. Harrigan, V. Schreiber, P. Stiegler, J. Piotrowski, L. Dawut, and V. A. Bohr.** 2004. Poly(ADP-ribose) polymerase 1 regulates both the exonuclease and helicase activities of the Werner syndrome protein. Nucleic Acids Res. **32:**4003–4014.
56. **von Kobbe, C., P. Karmakar, L. Dawut, P. Opresko, X. Zeng, R. M. Brosh, Jr., I. D. Hickson, and V. A. Bohr.** 2002. Colocalization, physical, and functional interaction between Werner and Bloom syndrome proteins. J. Biol. Chem. **277:**22035–22044.
57. **Von Kobbe, C., A. May, C. Grandori, and V. A. Bohr.** 2004. Werner syndrome cells escape hydrogen peroxide-induced cell proliferation arrest. FASEB J. **18:**1970–1972.
58. **von Zglinicki, T.** 2002. Oxidative stress shortens telomeres. Trends Biochem. Sci. **27:**339–344.
59. **Ward, I. M., K. Minn, K. G. Jorda, and J. Chen.** 2003. Accumulation of checkpoint protein 53BP1 at DNA breaks involves its binding to phosphorylated histone H2AX. J. Biol. Chem. **278:**19579–19582.
60. **Wyllie, F. S., C. J. Jones, J. W. Skinner, M. F. Haughton, C. Wallis, D. Wynford-Thomas, R. G. Faragher, and D. Kipling.** 2000. Telomerase prevents the accelerated cell ageing of Werner syndrome fibroblasts. Nat. Genet. **24:**16–17.
61. **Yang, H. S., and P. W. Hinds.** 2003. Increased ezrin expression and activation by CDK5 coincident with acquisition of the senescent phenotype. Mol. Cell **11:**1163–1176.